AD A132 735 A GALERKIN-FINITE ELEMENT TECHNIQUE FOR SMALL-SCALE 1/1
ATMOSPHERIC FLOWS AND..(U) COLORADO UNIV AT BOULDER
R L SANI 30 AUG 83 153-1836 ARO-15810.9-GS
UNCLASSIFIED DAAG29-82-C-0010 F/G 12/1 NL

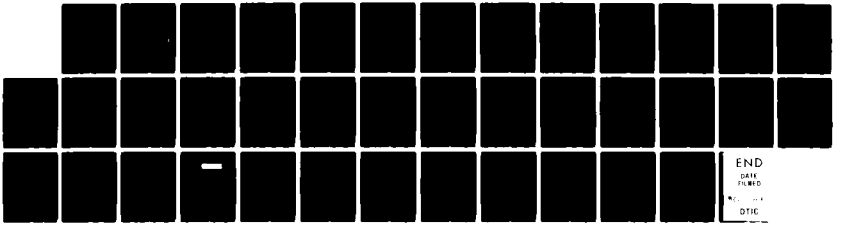

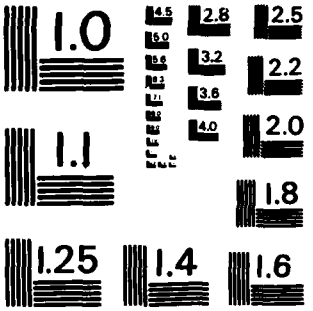

UNCLASSIFIED
SECURITY CLASSIFICATION OF THIS PAGE (When Data Entered)

ARO 15810.9-GS (12)

A182 735

REPORT DOCUMENTATION PAGE

READ INSTRUCTIONS BEFORE COMPLETING FORM

1. REPORT NUMBER	2. GOVT ACCESSION NO. / 3. RECIPIENT'S CATALOG NUMBER
4. TITLE (and Subtitle): A Galerkin-Finite Element Technique For Small-Scale Atmospheric Flows And Transport Over General Terrain	5. TYPE OF REPORT & PERIOD COVERED: Final Report 1979-1983
	6. PERFORMING ORG. REPORT NUMBER: 153-1836
7. AUTHOR(s): R. L. Sani	8. CONTRACT OR GRANT NUMBER(s): DAAG29-79-G-0045, DAAG29-82-C-0010
9. PERFORMING ORGANIZATION NAME AND ADDRESS: Dept. Chem. Engng & CIRES, University of Colorado, Boulder, CO 80309	10. PROGRAM ELEMENT, PROJECT, TASK AREA & WORK UNIT NUMBERS
11. CONTROLLING OFFICE NAME AND ADDRESS: U. S. Army Research Office, Post Office Box 12211, Research Triangle Park, NC 27709	12. REPORT DATE: August 30, 1983 / 13. NUMBER OF PAGES: 36
14. MONITORING AGENCY NAME & ADDRESS (if different from Controlling Office)	15. SECURITY CLASS. (of this report): Unclassified / 15a. DECLASSIFICATION/DOWNGRADING SCHEDULE

16. DISTRIBUTION STATEMENT (of this Report)

Approved for public release; distribution unlimited.

DTIC ELECTE SEP 21 1983 S D E

17. DISTRIBUTION STATEMENT (of the abstract entered in Block 20, if different from Report)

NA

18. SUPPLEMENTARY NOTES

The view, opinions, and/or findings contained in this report are those of the author(s) and should not be construed as an official Department of the Army position, policy, or decision, unless so designated by other documentation.

19. KEY WORDS (Continue on reverse side if necessary and identify by block number)

Galerkin-Finite Element
Small-Scale Atmospheric Flows
Navier-Stokes Equations
Boussinesq Equations

20. ABSTRACT (Continue on reverse side if necessary and identify by block number)

The development of a consistent penalty - Galerkin finite element algorithm for small-scale atmospheric flows over complex terrain is summarized. Various aspects of the development such as pressure smoothing, the development of an appropriate variable step time integrator, and appropriate outflow boundary conditions are discussed and pertinent references cited. Illustrative simulations are presented.

DTIC FILE COPY

DD FORM 1 JAN 73 1473 EDITION OF 1 NOV 65 IS OBSOLETE

UNCLASSIFIED
SECURITY CLASSIFICATION OF THIS PAGE (When Data Entered)

83 09 20 010

A GALERKIN-FINITE ELEMENT TECHNIQUE FOR SMALL-SCALE ATMOSPHERIC FLOWS AND TRANSPORT OVER GENERAL TERRAIN

Final Report

R. L. Sani

August 30, 1983

U. S. Army Research Office

Grant No. DAAG29-79-G-0045
Contract No. DAAG29-82-C-0010

Department of Chemical Engineering
University of Colorado
Boulder, CO 80309

The view, opinions, and/or findings contained in this report are those of the author and should not be construed as an official Department of the Army position, policy, or decision, unless so designated by other documentation.

PROBLEM DESCRIPTION

Introduction

There are many problems of interest to fluid dynamicists as well as meteorologists which require a small-scale, or limited area, model of flow and possibly concomitant transport of energy and species over irregular terrain. For example stratified flow over hills, or cities, and the associated transport of pollutants or atmospheric boundary layer studies in which the resolvable horizontal and vertical scales are of the same order of magnitude and the hydrostatic approximation is invalid. Considerable progress has been made in developing numerical techniques to simulate models of stratified flows without topography but the inclusion of general topographic effects has only recently received a thorough consideration from a numerical simulation, as well as operational standpoint, by, for example, Gal-Chen and Somerville (1975), Clark (1977), Mason and Sykes (1979 a, b), Mahrer and Pielke (1975, 1977) and Haussling (1977). The latter authors employ a terrain-following coordinate system which maps the irregular domain into a rectangular domain and then develops finite difference stencils for the various terms appearing in the transformed balance equations which must be satisfied by the primitive variables. Many of the aspects of these modeling efforts are reviewed in Pielke (1981).

The main thrust of our ARO sponsored research effort is the development and assessment of a primitive variable, non-hydrostatic Galerkin-finite element technique which can accommodate general topography, is capable of automatically generating a spatial discretization which conserves certain global quantities if desired (Lee, Gresho, Chan, Sani and Cullen (1981)) and is robust enough to handle very complex flows. We have developed and assessed the potential of a Galerkin finite element penalty technique for flow and transport problems, and, I believe, have clearly demonstrated its potential in satisfying the above

requirements.

BASIC DESCRIPTION OF PROTOTYPE SYSTEM AND TECHNIQUE

In order to simplify the discussion of the important features of the proposed technique the anelastic model used by Gal-Chan and Somerville (1975) will be used. (More complicated anelastic models with higher order turbulence closure schemes are compatible with the technique but of questionable utility in 3-D simulation on current generation computers.) The basic mathematical model is:

$$\nabla\cdot(\rho_0\mathbf{u}) = 0 \tag{1}$$

$$\frac{\partial(\rho_0\mathbf{u})}{\partial t} + \nabla\cdot(\rho_0\mathbf{uu}) = -\nabla p + \rho\mathbf{g} + \nabla\cdot\tau \tag{2}$$

$$\frac{\partial(\rho_0\varphi)}{\partial t} + \nabla\cdot(\rho_0\mathbf{u}\varphi) = \nabla\cdot\mathbf{H} \tag{3}$$

Here τ and $\mathbf{H}$ are respectively, the stress tensor and heat flux which, in general, are nonlinear functions of the local state of the flow. The Coriolis effect has been neglected but is easily included.

In applying a finite difference (FD) method these equations are usually transformed to a terrain following coordinate system and a discretized version is generated. In effecting the latter oftentimes a diagnostic pressure equation is generated and also discretized. In many cases the discretized version of the diagnostic pressure equation is rather complicated and its solution involves some sort of iteration scheme. One of the interesting features of the penalty Galerkin-finite element (PGFEM) technique proposed here is that the basic discretized system is one which only involves nodal velocities and the nodal pressures are obtained by post-processing of the nodal velocities. The basic idea appears to be due to Lions (1972) and belongs to the same family of slightly compressible approximations first introduced by Chorin (1967) but is not identical and is implemented here in a completely different manner. The

standard GFEM approach to anelastic fluid mechanical systems would involve interpolating both the velocity and pressure fields and generating nodal equations as outlined in a subsequent section. In a mixed scheme both nodal pressures and velocities appear as unknowns, not necessarily at each node since it is necessary to interpolate the pressure field with a lower order polynomial than the velocity field to obtain a well-posed algebraic problem for the nodal unknowns. (See, for example, Taylor and Hood, 1973; and Sani, Gresho and Lee (1980), Sani, Gresho, Lee and Griffiths (1981a), Sani, Gresho, Lee, Griffiths and Engelman (1981b).

In order to introduce the proposed penalty GFE, i.e. PGFE, technique one introduces the following perturbed system.

$$\nabla\cdot(\rho_0\mathbf{u}_\varepsilon) = -\varepsilon p_\varepsilon , \tag{4}$$

$$\frac{\partial(\rho_0\mathbf{u}_\varepsilon)}{\partial t} + \nabla\cdot(\rho_0\mathbf{u}_\varepsilon\mathbf{u}_\varepsilon) - \frac{1}{2}\{\nabla\cdot(\rho_0\mathbf{u}_\varepsilon)\}\mathbf{u}_\varepsilon = -\nabla p_\varepsilon + \rho\mathbf{g} + \nabla\cdot\tau_\varepsilon , \tag{5}$$

$$\frac{\partial(\rho_0\varphi_\varepsilon)}{\partial t} + \nabla\cdot(\rho_0\mathbf{u}_\varepsilon\varphi_\varepsilon) - \frac{1}{2}\{\nabla\cdot(\rho_0\mathbf{u}_\varepsilon)\}\varphi_\varepsilon = \nabla\cdot\mathbf{H}_\varepsilon \tag{6}$$

in which ε, the "penalty parameter", appears as a small perturbation parameter. By using the results of Teman (1968, 1976) and placing some modest restrictions on the form of τ and $\mathbf{H}$ it appears possible to formally establish that the two systems differ by an $0(\varepsilon)$ error which, of course, implies that the two systems (1)-(3) and (4)-(6), are identical as $\varepsilon\to 0$. The addition of terms involving $\frac{1}{2}\nabla\cdot(\rho_0\mathbf{u}_\varepsilon)$ insure that the discretized version of the advection terms is conservative (up to time truncation errors) and Lions (1972) has shown that these terms can be added without jeopardizing the accuracy of the method as long as ε is sufficiently small. The implication of these terms has been assessed in one aspect of the work initiated under the current research effort Lee, Gresho, Chan, Sani and Cullen (1981)). It was found that the GFE, or the PGFE, method is relatively insensitive (compared to a FD method) to the inclusion of these

terms to obtain a flux divergence form of the equations; however, the computation of derived quantities can be greatly effected (Gresho, Lee and Sani (1981)) and hence we routinely employ the flux divergence form.

The PGFE method utilized in our current algorithm leads to a formulation in which the nodal pressure variables do not explicitly appear -- a cost effective version of the general technique. It is noteworthy that our implementation does not formally replace p before discretizing via the GFE which, as is well-known, generates a "penalty term", $\frac{1}{\varepsilon}\nabla(\nabla\cdot\mathbf{u})$ which must be "underintegrated" when discretized by Galerkin's method, but directly discretizes the perturbed continuum equations via GFE using a C^{-1} finite element pressure representation. The latter results in a discretized approximation of the perturbed continuity equation which can be solved for nodal pressures at element level, a very efficient process. Whenever the nodal pressures within an element are desired they can be obtained by appropriate post-processing of the nodal velocities associated with the element. This PGFE method is referred to as a "consistent" penalty technique and its implementation and advantages are discussed in Engelman, Sani, Gresho and Bercovier (1981).

In the implementation of the scheme the approximate solution $(\tilde{\mathbf{u}},\tilde{p})$ is represented in the form

$$\tilde{\mathbf{u}}(x,t)=\sum_{j=1}^{N}\mathbf{u}_j(t)\varphi_j(x),\quad \tilde{p}(x,t)=\sum_{j=1}^{M}p_j(t)\psi_j(x) \tag{7}$$

The finite element basis set $\{\varphi_j(x)\}$ ($\{\psi_j(x)\}$) is nonzero only locally over a few elements (an element), i.e., is of local support, and φ_j (ψ_j) is unity at node j and zero at other nodes. (In certain cases it is convenient to relax the latter property for ψ_j.) The basis $\{\varphi_j(x)\}$ are required to be at least C^0 and the pressure basis $\{\psi_j(x)\}$ is required to be C^{-1} for efficient implementation of the technique. Both these choices are compatible with the weak form of the equations

associated with our Galerkin formulation which leads to a set of coupled first order ordinary differential equation of the form

$$\mathbf{M}\frac{d\mathbf{u}}{dt} + (\frac{1}{\varepsilon})\mathbf{B}\mathbf{u} + \mathbf{K}\mathbf{u} + \mathbf{A}(\mathbf{u})\mathbf{u} = \mathbf{b} \quad . \tag{8}$$

in which the matrices are sparse and usually banded but, in general, the bandwidths are much larlarger than the corresponding system generated by a regular finite difference stencil. This property implies that for the PGFEM to be competitive with a FD method fewer nodal unknowns must be used to achieve a specified accuracy and efficient storage and solution techniques must be utilized. The current state of GFEM (or PGFEM) development is such that very few documented comparisons between the GFEM and FD schemes are available in the literature but some preliminary coarse mesh comparisons of the schemes in simulating flow and advection-diffusion were encouraging (Gresho, Lee and Sani (1980)). The cost-effectiveness is important and an area of current research; *however, robustness is also a very important attribute and a recent test problem* (de Vahl Davis and Jones (1981)) points out the superiority of Galerkin finite element techniques in this regard.

The appearance of the non-diagonal mass matrix $\mathbf{M}$ in (8) implies the implicit character of the technique; in non-penalty Galerkin finite element techniques a so-called lumped version which replaces $\mathbf{M}$ by a diagonal matrix can often be effectively used but here with $(\frac{1}{\varepsilon})>>1$ an explicit scheme is inappropriate because of very stringent stability limitations, i.e., $\Delta t \sim 0(\varepsilon)$ and typically $\varepsilon \sim 10^{-6} - 10^{-8}$. In fact, there is a false transient induced by the method (a ramification of the singularity of $\mathbf{B}$ and smallness of ε) which must be dealt with properly. These points are discussed in more detail in the Summary of Results Section.

SUMMARY OF RESULTS

The emphasis in the program from its inception has been one of development coordinated with theory. Our initial study focused firstly, on understanding and implementing the penalty technique and secondly, on the ability of the technique to generate accurate solutions to difficult problems. During the course of the study detailed investigations were carried out on (1) spurious pressures and consistent penalty in simulation of incompressible media; (2) the "false transient" associated with the consistent penalty technique and the design of a variable step time integration with local error control to cope with this problem in a cost-effective manner; (3) the generation and evaluation of new elements; (4) the derivation of "consistently" derived normals on the boundary of a computational domain which is represented in the GFE method by a C^0 representation; (5) initial studies of turbulence parameterization; (6) the development of pre- and post- processing techniques; (7) benchmark simulations assessing and illustrating features of the technique. Since these studies have formed the basis of the published manuscripts cited in the Publications Section and are readily available, only the highlights of certain aspects are presented here.

1. Spurious Pressures and Consistent Penalty formulation

Discretized approximations to the incompressible Navier-Stokes equations, in the primitive variable (velocity-pressure) formulation, especially when generated via the Galerkin finite element method (GFEM), have been plagued with confusion regarding the 'appropriate' workable combinations of velocity and pressure approximations. Early on it was discovered by Hood and Taylor (1973) that equal-order interpolation on conforming quadrilateral elements, wherein the same basis functions are used for representing velocity and pressure, causes difficulty in the pressure solution. They obtained better results when

using mixed interpolation (the basis functions for pressure were one order lower than those for velocity), and suggested an explanation in the form of "balancing residuals" from momentum and continuity equations. Their explanation, although intuitively appealing, was judged inadequate by Olson and Tuann (1978) who explained the results in terms of the eigenvalues of a single element (equal interpolation always generated one or more eigenvectors which contained only pressure and corresponded to zero eigenvalues; they claimed that these were spurious and were the cause of the failure).

Even when mixed interpolation is employed, however, there are cases where numerical difficulties are encountered. In particular, the simplest possible approximation employs piecewise linear approximation for velocity (bilinear on quadrilaterals) and piecewise constant approximation for pressure. This element has been found to work well in some cases and poorly in others; in solid mechanics, see Argyris et al (1974) and Nagtegaal, Parks and Rice (1974), and in fluid mechanics, see Fabayo (1977), Huyakorn et al (1978), Hughes, Liu and Brooks, (1979), and Lee, Gresho and Sani (1979). For certain combinations of boundary conditions and element distributions over a domain, the solutions display acceptable velocities but totally spurious pressures; the pressures are afflicted with the "checkerboard syndrome," wherein they display oscillations which are frequently of one sign on all 'black' squares and of the opposite sign on all 'red' squares. These pressure patterns have also been encountered using certain finite difference discretization techniques (Fortin (1972), Pracht and Blackbill (1976) so that the affliction is not intrinsic to GFEM formulations; for example, Chorin (1969) has encountered four spurious pressure patterns when solving a consistently centered difference approximation to the Navier-Stokes equations in two-dimensions (eight in 3-D). Finally, similar behavior can also occur using higher-order elements; e.g. the quadrilateral element with biqua-

dratic velocity (9-node) and bilinear pressure with nodes at the 2 x 2 Gauss points can display a checkerboard syndrome.

In the related penalty method (PGFEM) which is of interest herein, the solenoidal constraint on the velocity field is slightly weakened, to $p = -\lambda \nabla \cdot \underline{u}$, where $\lambda = (\frac{1}{\varepsilon})$ is the penalty parameter. The results from the penalty approximation will be close to those using (1b) if the following inequalities are satisfied: $\varepsilon << \mu/\lambda << 1$, where ε is the "unit roundoff level" of the computer; for example, on our CDC-720, $\varepsilon \approx 10^{-14}$ and the penalty method 'works well' for $\approx 10^{5} < \lambda/\mu < \approx 10^{9}$. With perfect arithmetic ($\varepsilon = 0$), the penalty results would converge to those from (1) as $\lambda \rightarrow \infty$. For large but finite λ, the results should typically differ by $0(1/\lambda)$; actually, we usually observe ≈6 digits of agreement for $10^{6} \leq \lambda \leq 10^{8}$. Since the pressures obtained from the penalty method can also be plagued with the checkerboard syndrome, it is appropriate to consider it also.

It is shown in Sani et al (1981 a, b) that the spurious pressures are ramifications of non-physical elements in the null space of the discretized pradient operator, i.e., solution to the GFEM discretized form of (4) - (5) is of the form $(\mathbf{u},p) = (0,\hat{p})$ where $\hat{p}$ is not a constant vector. The consequences and filtering of these spurious pressures on regular as well as isoparametric meshes is discussed in the above references. As alluded to above the penalty method advocated herein is **theoretically** devoid of spurious pressures but, in fact, finite precision numerical simulations using certain elements can exhibit oscillations ***but*** usually of very small amplitude. If desired these oscillations may also be filtered by techniques alluded to above. However, in most cases one can select velocity-pressure approximations which do not exhibit such spurious pressures, and for example, in 2D the biquadratic velocity-linear pressure interpolant which we reported in Engelman et al (1982) appears to be an optimal

combination.

An example comparing "filtered pressures" from a biquadratic C^0 velocity - linear C^{-1} pressure element mixed mode simulation with the unfiltered pressures from the consistent penalty approach advocated herein using the same element pair as well as a bilinear C^0 velocity - piecewise constant C^{-1} pressure element is illustrated in Figure 1.

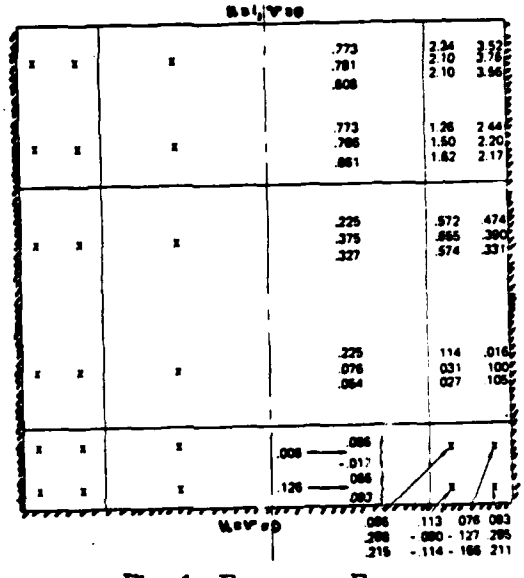

Fig. 1. Pressure From
A Driven Cavity Experiment

Since the mesh is symmetric, and the "penalty" pressures satisfy $\int_\Omega p^h = 0$ only one-half of the pressures are displayed; the pressures at the Gauss points in each element shown on the left side are the negative of those printed on the right side. For the mixed interpolation case, the spurious pressure was first filtered, then the hydrostatic level was adjusted to agree with that from the penalty case. The first entry at each "node" is that from mixed interpolation; the second entry is the 9-node penalty pressure, and the bottom entry is the 4-node penalty pressure.

It is apparent in Figure 1 that all pressures look fairly reasonable in the

high pressure region and, considering the coarseness of the mesh, agree quite well with each other. The differences show up in the low pressure region wherein a "lingering local pressure oscillation is present in both penalty results. Finally, as mentioned earlier, if the 9-node penalty pressures are filtered, the resulting pressures agree with the filtered mixed interpolation pressures to $\approx O(1/\lambda)$ and are the physical pressures in the sense that they are the only ones "seen" in the momentum equations. The latter pressure would have been obtained *without* filtering by employing a linear C^{-1} pressure interpolant initially - a ramification of the optimality of this element.

A detailed theoretical discussion of the filtering schemes as well as additional numerical examples are presented in Lee, Gresho and Sani (1979); moreover, a detailed discussion of the Galerkin-finite element penalty method is presented. It is noteworthy that the implementation of the technique herein is via the "consistent penalty method" and not the popular under-integration implementation most often employed in the engineering literature. While the two techniques may be equivalent on a rectangular mesh there can be significant differences on isoparametric meshes composed of generalized quadrilaterals. The latter is illustrated in Table 1, detailed in Engelman, Sani, Gresho and Bercovier (1982) and represented an important contribution of our initial investigation. One of the benchmark simulations used in generating a comparison of the methods was a "colliding flow". In this flow, fluids flow from $+y_\infty$ and $-y_\infty$ to collide at $y = 0$. The solution over the entire x-y plane is

$$u_x = Cx$$
$$u_y = -Cy$$
$$p = -\frac{C}{2}\rho(x^2 + y^2)$$

The region $0 \le x \le 1, 0 \le y \le 1$ was modeled with symmetry planes (zero normal velocity and tangential stress) prescribed along $x = 0$ and $y = 0$ and the exact solu-

tion along $x = 1$ and $y = 1$. The parameters used were $C = 4$, density $\rho = 1$ and viscosity $\mu = .0667$.

The approximate solution to each problem was obtained using both the reduced integration and the consistent construction of the penalty matrix for $p \varepsilon Q_1$ and $p \varepsilon P_1$ on three different meshes. The meshes were: a regular 6x6 mesh of nine node squares, a 6x6 mesh of irregular quadrilaterials, and a 6x6 mesh of curved isoparametric elements. The isoparametric mesh was generated by moving each mid-side node inwards or outwards a distance of 5% of the element width. The results of the simulation are presented in Table 1. They are in complete agreement with the theoretical predictions; that is, on both the regular and distorted quadrilateral meshes both the reduced and consistent constructions of the penalty matrices give essentially identical solution errors. It is only on the curved isoparametric meshes that the differences between the reduced and consistent formulations manifest themselves. Here we see a large error in the pressure solution when reduced integration is used which decreases markedly when a consistent construction is employed. Only the results for the isoparametric mesh are reported in Table 1, as the regular and quadrilateral meshes gave nearly identical errors for all three formulations.

Mesh	Pressure Formulation	Rel. Error Velocity	Rel. Error Pressure
Isoparametric Elements	Reduced Integration $p \varepsilon Q_1$	.05057	.02384
	Consistent $p \varepsilon Q_1$	.03185	.02129
	Consistent $p \varepsilon P_1$	.01876	.01601

Table 1: 2-D Colliding Flow Problem

2. False Transient Associated With The Penalty Technique.

The penalty method used in our small scale atmospheric model weakens the solenoidal constraint (1) to the weaker one (4). As a consequence, the infinite speed of propagation of a pressure signal in an incompressible fluid is replaced by an $0(\lambda)$ "diffusive" speed of propagation - a property which can lead to a non-physical transient. Here $\lambda \equiv 1/\varepsilon$ and $\varepsilon << 1$. Since the penalty parameter is large, the initial nonphysical transient is fast, occurring on a time scale of $0(1/\lambda)$, and reflects the slight compressibility inherent in the weakened solenoidal constraint. While the analogy with a "special" slightly incompressible fluid has been noted by others, it appears that the associated non-physical transient has received little attention in the literature. In Sani et al (1981c) attention focused on the existence, characterization and remedy of the initial non-physical portion of the transient associated with a well-posed (in the incompressible sense) problem and also illustrate the physically uninteresting transient associated with an ill-posed problem. The nature of the false transient can be demonstrated by considering the development of a Poisieulle flow.

Using the mesh and boundary conditions shown in Figure 2 and starting with the fluid at rest, i.e., $u = v = o$, then the time histories shown in Figure 3 are obtained. The curves labeled "mixed" are obtained using the solenoidal constraint (1) and can be considered as the exact physical behavior. It is clear that a rapid, non-physical penalty transient occurs on a time scale of $0(\varepsilon)$ after which the penalty methods tracks the physical transient.

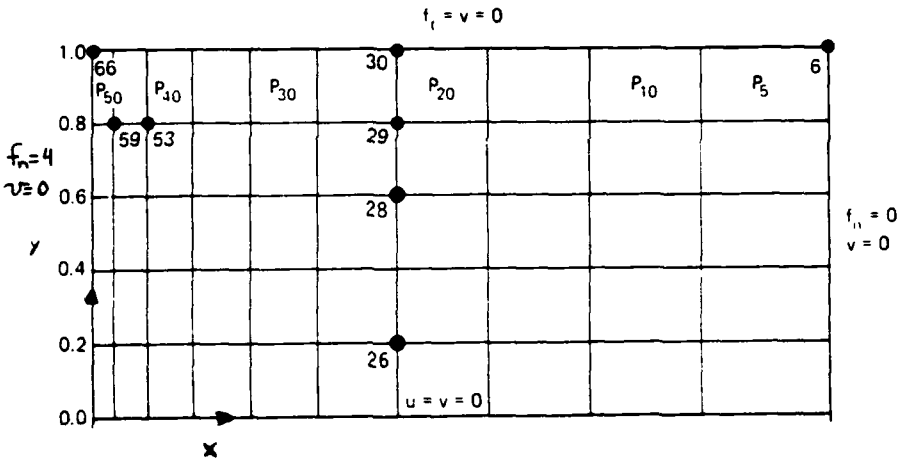

Fig. 2. Mesh and Boundary Conditions

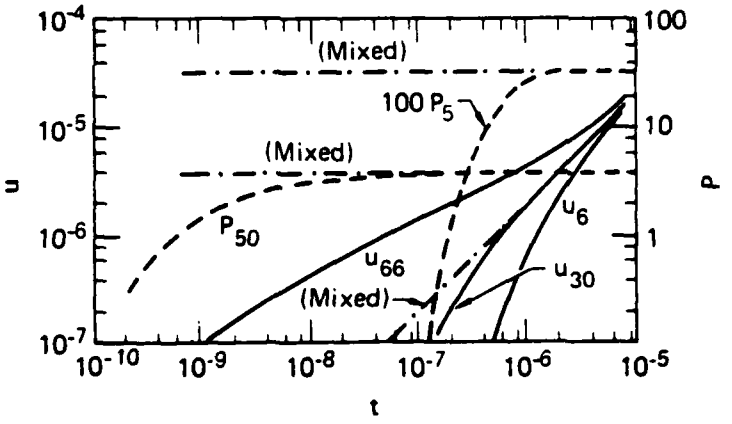

Fig. 3. Selected Time Histories
During Penalty Transient

Since the penalty parameter, λ, is very large, it can be shown that an explicit time integration algorithm leads to time steps (Δt) of $0(1/\lambda)$ for stability - an unacceptable restriction imposed by the non-physical part of the transient. Even implicit algorithms which are non-dissipative can be severely limited in time step size; for example, if the trapezoid rule algorithm is chosen, undamped oscillations will occur if $\lambda\Delta t$ is much greater than unity. Consequently, a time integrator was designed with the capability of starting out in a constant, or variable, Δt backward Euler (BE) mode (an implicit, first-order, dissipative scheme) and switching to a variable Δt BE mode or trapezoid (TR) mode (an implicit, second-order, non-dissipative scheme) after a preassigned number of time steps. Using this algorithm one can either follow the *entire* transient to within a prescribed local time truncation accuracy via a variable step method exclusively, or follow only the *physical* part of the transient by initially taking a few BE steps at a constant $\Delta t \gg (1/\lambda)$ and then switching to variable step BE or TR for efficiency. The initial non-physical portion of the transient appears as "high frequency signals" to the BE scheme and is therefore quickly damped by the numerical diffusion associated with this scheme. Consequently, this stable time integration strategy can **over-look** the initial non-physical transient while using reasonable-sized time steps, i.e., time steps **not** $0(\varepsilon)$, and can be up to second order accurate in the remaining (physical) portion of the transient while automatically varying Δt, based solely on temporal accuracy requirements. The details are reported in Sani et al (1981c) and the basic ideas can be exploited by others in other applications.

3. Consistently Derived Boundary Normals

It is often required to specify normal, or tangential, velocities along the boundary of a domain, or equivalently along the element boundaries forming the finite element covering of a domain. In general, these boundaries are not

along level surfaces of the coordinate system for the problem. For example, in modeling flows with free surfaces such as the ocean-atmosphere interaction or in raising the computational domain "off the ground" when assuming the lowest level flow is well represented by a locally equilibrium log-linear profile. We addressed this issue in Engelman, Sani and Gresho (1982) where a detailed analysis is presented and it is shown that if the normal vector computation is not done in a manner consistent with the incompressibility constraint, erroneous results, especially in pressure, can result.

4. Outflow Boundary Conditions

During our study it was demonstrated mainly by numerical experiment that appropriate computational outflow boundary conditions for *neutral and special stratified* flows could be obtained by using the "natural" boundary conditions associated with the Galerkin formulation, i.e., constant normal, f_n, and in some cases tangential f_t, stress on an outflow boundary. (Here $f_n = \mathbf{nn}:\tau$ and $f_t = \mathbf{tn}:\tau$.) While these conditions are not generally physically correct for the continuum system (outflow boundaries imposed by the requirements of a bounded computational domain are unphysical and apriori the "correct" boundary conditions are unknown) benchmark numerical experiments indicate that such boundary conditions lead to accurate interior numerical results especially in advection dominated cases. For example, in the simulation of the shedding of a von Karmen vortex street at Re = 110 shown in Figure 4, the outflow boundary conditions for this neutral flow were $f_n = 0$, $f_t = 0$. Notice that the vortex street leaves the computational domain without noticeable mesh effects.

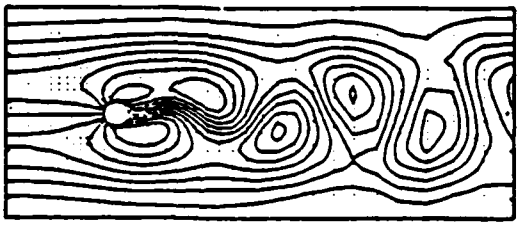

Fig. 4. Relative Streamlines As Seen By An Observer Moving With The Nominal Fluid Velocity

It is also noteworthy that the **weak** form of the boundary constraint $f_n = const.$ is not enforced locally but in a least square error sense over the outflow boundary; only in the limit of zero mesh size is the constraint imposed locally. It is the latter feature that makes this **natural** boundary condition which allows **u** and **p** to be computed *on the outflow* boundary a good computational outflow boundary condition. The variation of f_n and $-p$ on the outflow boundary of the vortex shedding numerical experiment at a specific time is displayed in Figure 5.

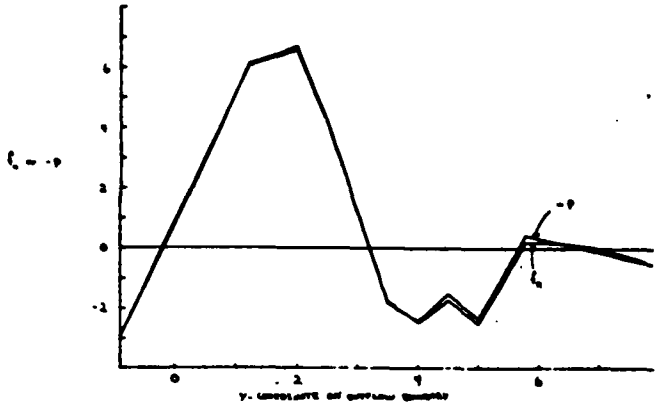

Fig. 5. f_n and $-p$ On Outflow Boundary At t = 536.49

It is noteworthy that $f_n \approx -p$ since on this outflow boundary

$$f_n = -p + 2\mu \frac{\partial u}{\partial x}$$

which shows that even at Re = 110 the viscous effects at the outflow boundary are small and also that in a **strong** sense $fn \neq const.$ which would be inappropriate physically.

While the solution to the problem of appropriate outflow boundary conditions appears to be reasonably resolved for neutral flows with small Coriolis effects, the solution in the case of many stratified flows and/or flows with significant Coriolis effects requires a more careful analysis. It is easily demonstrated by exact solutions as well as numerical experiments that setting, for example, $f_n = const.$, in such flows leads to the solution of a **different problem** than originally desired. The latter is a ramification of both velocity and pressure field contributions in the normal stress f_n coupled with the occurrence on the outflow boundary of a significant, apriori unknown, pressure contribution due mainly to hydrostatic pressure variations in a stratified flow and/or pressure variations due to Coriolis effects in a rotating flow. (Centrifugal can be handled

by a redefinition of the pressure variable to include such effects.)

The solution to this outflow boundary condition problem is being dealt with by using a **natural** boundary of the form

$$2\mu \frac{\partial u_n}{\partial n} = const.$$

which again is not **physically** correct pointwise but is only satisfied in a weak sense and leads to an acceptable computational outflow boundary condition except in the case of a piecewise constant pressure interpolant where a special f_n updating procedure must be used. While the formal implementation of the boundary condition is straightforward there are certain theoretical as well as computational question which must be addressed in order that a firm basis for its use is established; these issues are addressed in Engelman, Sani and Gresho (1982) and form the basis of some ongoing research. Its use will be illustrated subsequently in one of the examples in the Benchmark Simulation Section.

5. Benchmark Simulations

During the course of this study a number of numerical experiments were performed in order to check the basic algorithm as well as to judge the viability, effectiveness and robustness of new techniques during the course of their implementation and development. These simulations varied from the simplest for which the algorithm was capable of generating an exact solution to complicated transient stratified flows in complex domains. The results of some of these numerical experiments are presented here in order to illustrate the capability of the algorithm as well as some of the pre- and post-processing techniques which were either developed during this study or scavenged from existing algorithms.

In all the following examples illustrating the capabilities of the algorithm a C^0 biquadratic velocity - C^{-1} linear pressure element, i.e., interpolation, is

employed in the PGFEM using $\varepsilon = 10^{-6}$. Isoparametric elements were used to grade the mesh and to track the complex geometry. (Each element appearing in the following figures illustrating the mesh contain 18 velocity degrees of freedom and 3 pressure degrees of freedom.)

1. Steady, Slow Neutral Flow Over A Circular Trench

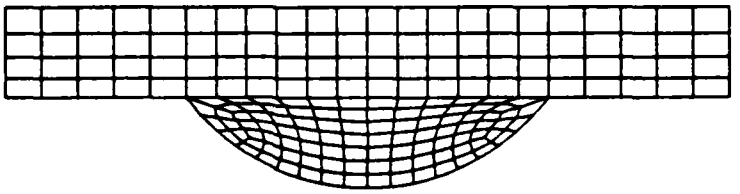

Fig. 6a. Mesh

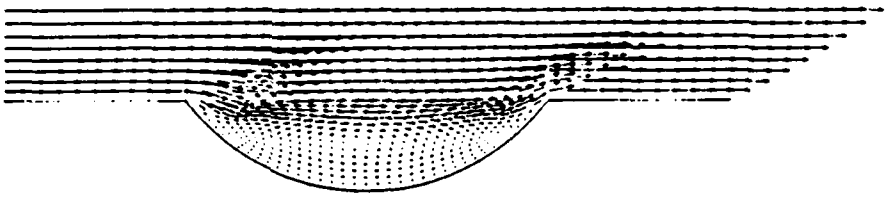

Fig. 6b. Velocity Vectors

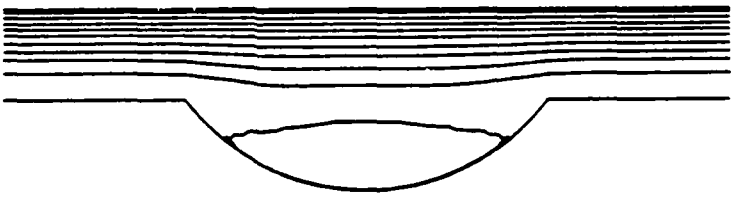

Fig. 6c. Streamlines

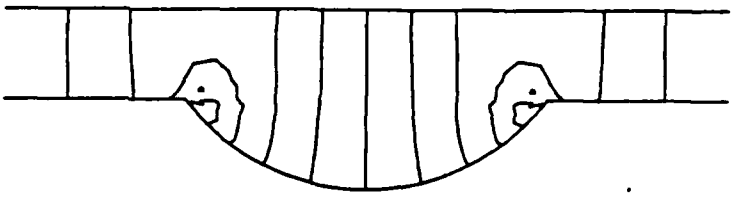

Fig. 6d. Isobars

The noteworthy features here are (i) the ability to easily track geometry and grade the mesh to track the physics if known apriori; (ii) the quality of the solution in that it accurately predicts the recirculation zone in the bottom of the trench, a feature whose existence can be predicted theoretically and (iii) the fact that the pressure sigularities which theoretically exist at the points of intersection of the trench with the planar region and which are not approximated very accurately by the mesh being used only, effect the numerical solution in the neighborhood of the singularities.

2. Steady, Stably Stratified Flow Over Topography

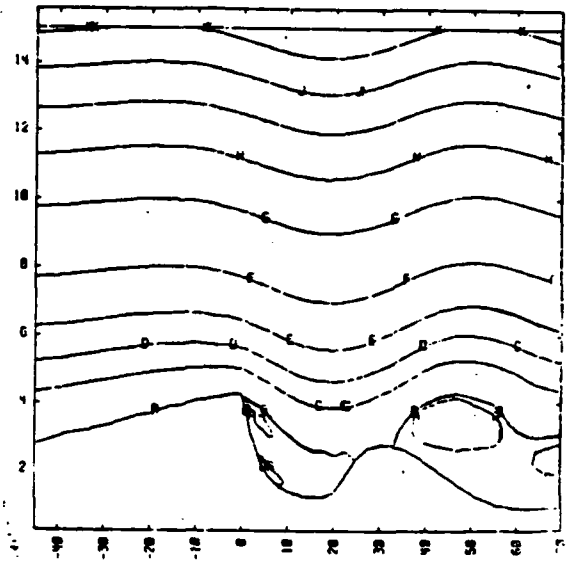

Fig. 7. Owens Valley Flow

This example illustrates a steady stratified flow with a Froude number, i.e., ratio of inertial to gravitational forces, of 4.5. For simplicity the simulation was done specifying a constant ground temperature and an inlet temperature profile which increased linearly with height and a specified inlet velocity field so that a comparison could be made with some simulations done previously by the group at Lawrence Livermore National Laboratory. The comparison was essentially exact and in both cases such features as mountain lee waves and up-slope winds are evident.

3. Transient Neutral and Stratified Flow About a Cylindrical Object

This flow was chosen because of the numer of experimental observations available in the literature, at least in the neutral flow case, for comparison. The details of the mesh and boundary conditions are displayed in Figure 1. (Note that the outflow bounding conditions illustrated are those appropriate to the neutral flow case.)

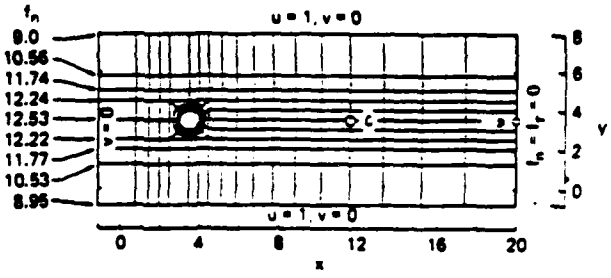

a. Overall domain, mesh, and boundary conditions.

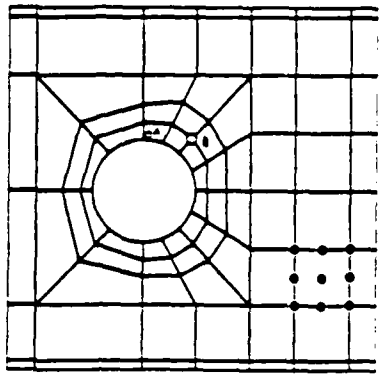

b. Details of mesh near cylinder; also shown are the nodes for a typical element.

Fig. 8. Mesh and Boundary Conditions

The numerical experiment started with the zero flow initially and the velocity field evolves to one at a Reynold's number of ≈ 100 (based on cylinder diameter) with a period shedding of a vortice, first from the top and then from the bottom of the cylinder. That is, a von Karmen vortex street develops behind the cylinder and flows out the computational domain. These features are illustrated in Figures 10-14. These predictions are in close agreement with observations made in physical experiments.

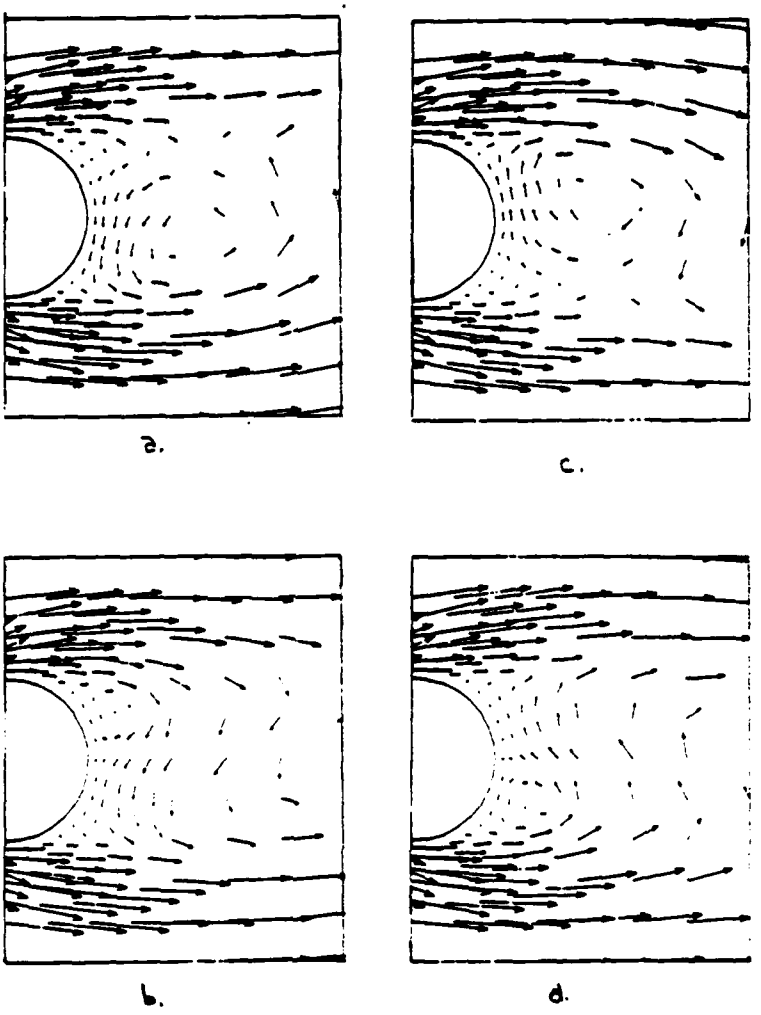

Fig. 10. Details of Vortex Generation During Quarter Cycle of Vortex Formation

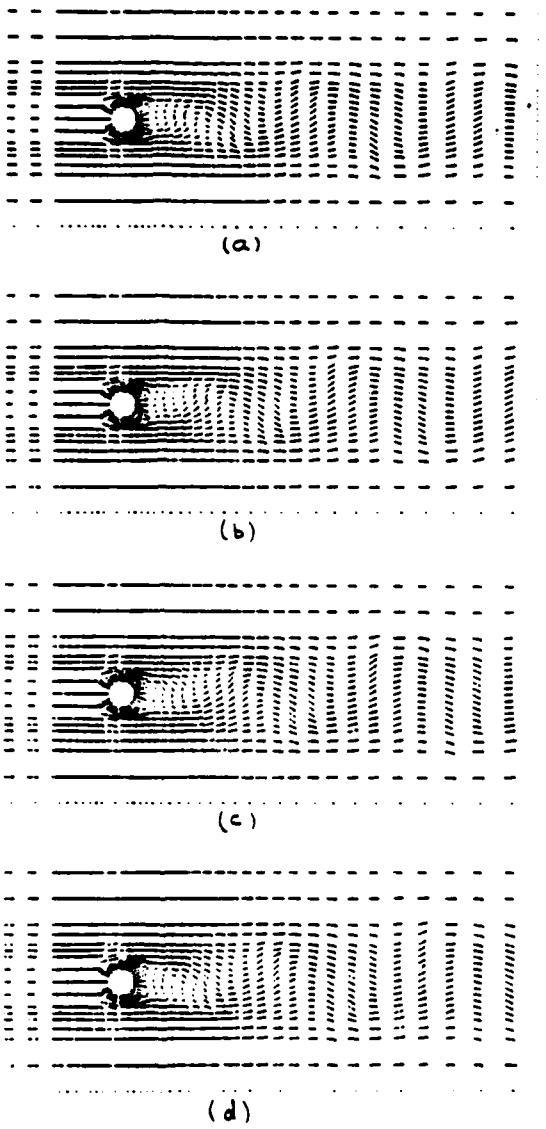

Fig. 9. Velocity Vectors During Quarter Cycle of Vortex Shedding.

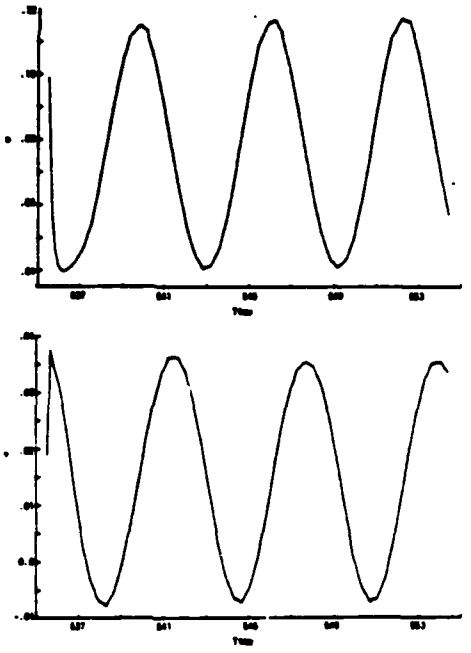

Fig. 11. Time History of
Velocity At Node B
During Shedding Cycle

The latter is also illustrated in Figures (12) - (13) where streaklines computed over a numerically simulated vortex shedding cycle (Figure 12) can be compared to those experimentally observed at a Reynolds number of 102, (Figure 13).

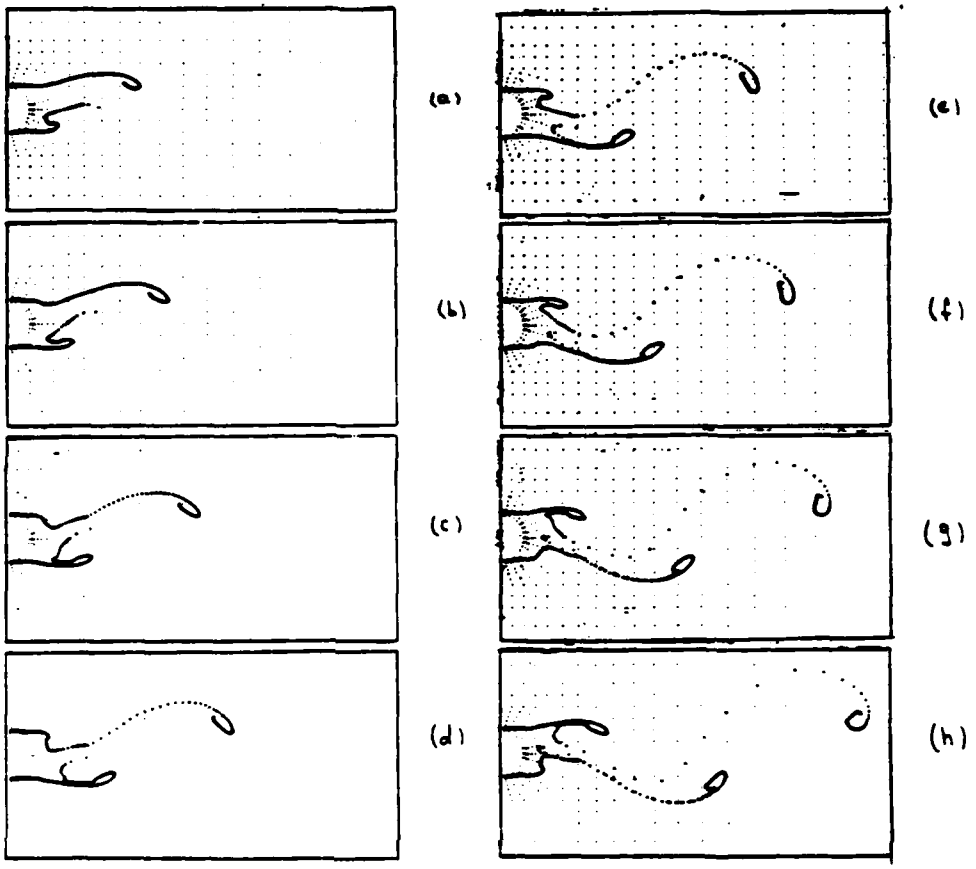

Fig. 12. Streaklines From Top And Bottom Of Cylinder At Interval of 1/8-th A Shed Cycle.

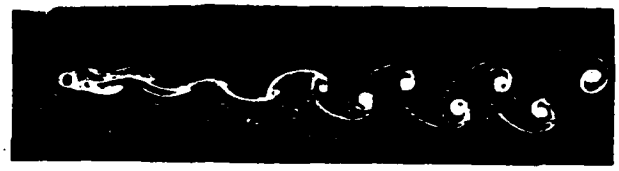

Fig. 13. Experimentally Observed Streakline

In the comparison one can focus on the "eye patterns" as they are swept downstream. The downstream movement of these patterns away from the centerline obvious in both the numerical and physical experiments and overall features compare very well. (The algorithm for computing the streaklines was developed during the course of our study and has been an aid in understanding some features of the flows as well as a starting point for tracking some neutrally buoyant particles.)

Finally to test the new outflow boundary conditions as well as to gain some insight into a stratified flow about an object the temperature of the cylinder was raised above that of the entering stream and the top and bottom boundaries were insulated. In our initial experiment the heating was minimal. The overall flow structure didn't change much except now the vortices leaving the cylinder are more asymmetric and have a tendency to raise during their downstream course. Moreover, the temperature field exhibits temporal oscillations as displayed in Figure 14.

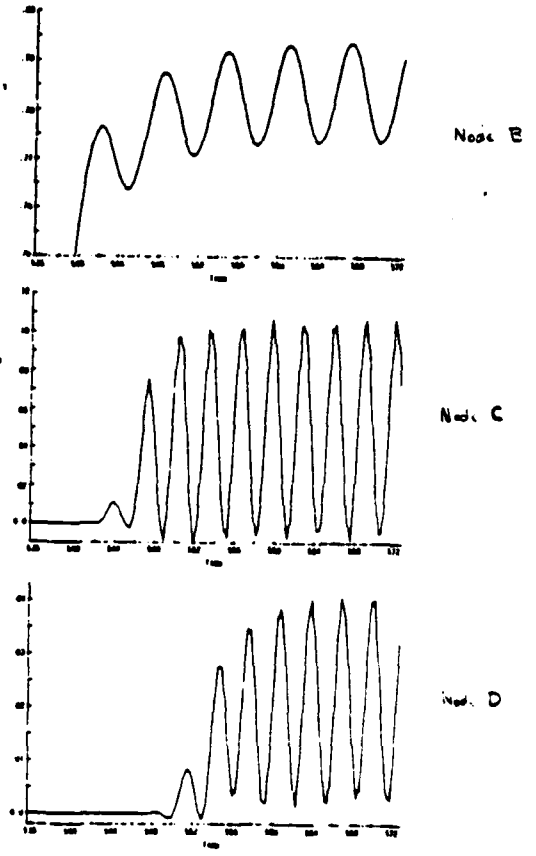

Fig. 14. Time History of Temperature
At Nodes B, C and D During
Shedding Cycle.

The new outflow boundary condition appeared to perform satisfactory with regard to the velocity field calculations but some difficulty was encountered in recovering an accurate pressure field; the latter has stimulated some ongoing research in this area.

PUBLICATIONS

1. "On The Spurious Pressures Generated By Certain GFEM Solutions Of The Incompressible Navier-Stokes Equations," Proc. 3rd Int. Conf. On Finite Elements In Flow Problems, Banff, Canada (1980).

2. "The Cause And Cure (?) Of The Spurious Pressures Generated By Certain FEM Solutions Of The Incompressible Navier-Stokes Equations," Part 1, Int. J. Number Methods in Fluids, 1, 17-43 (1981).

3. "The Cause And Cure (?) Of The Spurious Pressures Generated By Certain FEM Solutions Of The Incompressible Navier-Stoes Equations," Part 2, Int. J. Num. Methods In Fluids, 1, 71-204 (1981).

4. "A Diabatic, Turbulent Atmospheric Boundary Layer Model," Proc. 3rd Int. Conf. On FEM In Flow Problems," Banff, Canada (1980).

5. "A Finite Element Sea Breeze Model," Proc. 5th Sym. On Turbulence, Diffusion and Air Pollution, Atlanta, GA (1981).

6. "Numerical Simulation Of Transport Processes Using The Galerkin Finite Element Method." Proc. 3rd Int. Conf. Physics Chemical Hydrodynamics, Madrid, Spain (1980).

7. "The Consistent Method For Computing Derived Boundary Quantities When The Galerkin FEM Is Used To Solve Thermal And/Or Fluids Problems," Proc. 3rd Int. Sym. Num. Methods In Thermal Problems, Venice, Italy, Pineridge Press (1981).

8. "On The Solution Of The Time-Dependent Incompressible Navier Stokes Equations Via A Penalty Galerkin Finite Element Method," Proc. 3rd Int. Sym. Num. Methods In Laminar and Turbulent Flow Venice, Italy, Pineridge Press (1981).

9. "Consistent Vs. Reduced Integration Penalty Methods For Incompressible Media Using Several Old and New Elements," Int. J. Num. Methods In Fluids, **2**, 25-42 (1982).

10. "The Implementation Of Normal And/Or Tangential Boundary Conditions In Finite Element Codes For Incompressible Fluid Flow," Int. J. Num. Methods in Fluids **2**, 225-238 (1982).

11. "Conservation Laws for Primitive Variable Formulations Of The Incompressible Flow Equations Using The Galerkin Finite Element Method," Finite Elements In Fluids, **4**, Chapt. 2, John Wiley and Sons (1982).

12. "On The Solution Of The Incompressible Navier-Stokes and Boussinesq Equations Via A Penalty Galerkin Finite Element Method," Proc. 4th Int. Sym. On Finite Element Methods In Flow Problems, Tokyo (1982).

13. "An Exploratory Study On The Application Of An Existing Finite Element Navier-Stokes Code To Compute Potential Flows," Proc. Int. Conf. On Finite Element Methods, Shanghai (1982).

PARTICIPATING SCIENTIFIC PERSONNEL

1. Prof. R. L. Sani (Principle Investigator)
2. Mr. B. Eaton (Ph. D. candidate; doctoral thesis work completed; degree to be awarded Dec. 1983)
3. Mr. G. Hardin (Ph. D. candidate)
4. Dr. M. S. Engelman (Post-doctoral Research Associate)
5. Ms. A. Peskin (Ph. D. candidate)
6. Ms. A. Fredrickson (Senior Research Project for B. S. Degree In Chem. Eng.)
7. Ms. D. McKay-Perez (Senior Research Project for B.S. Degree in Chem. Eng.)
8. Ms. L. Logan (Senior Research Project for B. S. Degree in Chem. Eng.)

BIBLIOGRAPHY

1. Argyris, J. H., P. C. Dunne, T. Angelopoulos, and B. Bichat, Large Natural Strains and Some Special Difficulties due to Non-linearity and Incompressibility in Finite Elements, Comp. Math. Appl. Mech. and Eng., 4, 219-278 (1974).

2. Chorin, J., A Numerical Method For Solving Incompressible Viscous Problems, J. Comp. Phys., 2, 12-26 (1967).

3. Chorin, A., personal communication and, On the Convergence of Discrete Approximations to the Navier-Stokes Equations, Math. of Comp., 23, 341-353 (1969).

4. Clark, T. L., A Small Scale Dynamic Model Using A Terrain Following Coordinate Transformation, J. Comp. Phys. 24, 186-215 (1977).

5. de Vahl Davis, G. and I. P. Jones, Natural Convection In A Square Cavity - A Comparison Exercise, Proc. 3rd Int. Sym. Num. Methods in Thermal Problems, Venice, Italy, Pineridge Press (1981).

6. Engelman, M., R. L. Sani, P. M. Gesho and M. Bercovier, Consistent Vs. Reduced Integration Penalty Methods For Incompressible Media Using Several Old And New Elements, Int. J. Num. Methods In Fluids 2, 25-42 (1982).

7. Engelman, M., R. L. Sani, and P. M. Gresho, The Implementation of Normal and/or Tangential Boundary Conditions in Finite Element Codes for Incompressible Fluid Flow. Int. J. Num. Methods In Fluids 2, 225-238 (1982).

8. Fabayo, O. R., Bilinear Finite Elements for Incompressible Flow, M. Sc. Dissertation, Dept. Math., University of Dundee, Scotland (1977).

9. Fortin, M., Numerical Solution of Steady State Navier Stokes Equations, Numerical Methods in Fluid Dynamics, J. J. Smolderen (editor), Agard Lec-

ture Series No. 48, GARD-LS-48 (1972).

10. Gal-Chen, T. and R. C. J. Somerville, Numerical Solution of the Navier-Stokes Equations with Topography, J. Comp. Phys. 17, 276-310 (1975).

11. Gresho, P. M., R. L. Lee and R. L. Sani, The Consistent Method For Computing Derived Boundary Quantities When The Galerkin FEM Is Used To Solve Thermal And/Or Fluids Problems, Proc. 3rd Int. Sym. Num. Methods In Thermal Problems, Venice, Italy, Pineridge Press (1981).

12. Gresho, P. M., R. L. Lee and R. L. Sani, On the Time-Dependent Solution of the Incompressible Navier-Stokes Equations in Two and Three Dimensions, Recent Advances in Numerical Methods in Fluids, Pineridge Press, Ltd., Swansea, U. K., Chapt. 2, 27-80 (1980).

13. Haussling, H. J., Viscous Flow of Stably Stratified Fluids Over Barriers, J. Atm. Sci. **34**, 589-602 (1977).

14. Hughes, T. J. R., W. K. Liu, and A. Brooks, Finite Element Analysis of Incompressible Viscous Flows by the Penalty Formulation, J. Comp. Phys., **39**, 1-15 (1979).

15. Huyakorn, P. A., C. Taylor, R. L. Lee and P. M. Gresho, A Comparison of Various Mixed Interpolation Finite Elements in the Velocity-Pressure Formulation of the Navier-Stokes Equations, Computers and Fluids, **6**, 25-35 (1978).

16. Lee, R. L., P. M. Gresho and R. L. Sani, Smoothing Techniques for Certain Primitive Variable Solutions of the Navier-Stokes Equations, Int. J. Num. Methods in Engng., 14, 1785-1804, (1979).

17. Lee, R. L., P. M. Gresho, S. Chan, R. L. Sani and M. J. P. Cullen, Conservation Laws for Primitive Variable Formulations Of The Incompressible Flow Equations Using The Galerkin Finite Element Method, Chapt. 2, **Finite Elements In Fluids**, 4, John, Wiley and Sons (1981).

18. Lions, J. L., On the Numerical Approximation of Some Equations Arising In Hydrodynamics, AGARD Lecture Series #48, J. J. Smolderen (editor) (1972).

19. Mahrer, Y. and R. A. Pielke, A Numerical Study of the Airflow Over Mountains Using 2-D Version of Univ. Virginia Mesoscale Model, J. Atm. Sci. **32**, 2144-2155 (1975).

20. Mahrer, Y. and R. A. Pielke, Numerical Simulation of the Airflow Over Barbados, Mon. Weather Rev. **104**, 1392-1402 (1977).

21. Mason, P. J. and Sykes, R. I. Flow Over An Isolated Hill of Moderate Slope, Quart. J. Roy. Met. Soc. **1-5**, 383-394 (1979).

22. Mason, P. J. and Sykes, R. I., Three Dimensional Numerical Integrations of the Navier-Stokes Equations For Flow over A Surface-Mounted Obstacle, J. F. M. **91**, 433-450 (1979).

23 Mitchell, A. R. and R. Wait, **The Finite Element Method In Partial Differential Equations**, John Wiley and Sons (1977).

24. Nagtegaal, J. D., D. M. Parks and J. R. Rice, On Numerically Accurate Finite Element Solutions in the Fully Plastic Range, Comp. Math. Appl. Mech. and Eng., **4**, 153-177 (1974).

25. Pielke, R. A., Mesoscale Numerical Modeling, Adv. Geophysics, **23**, 185-344 (1981).

26. Pracht, W. E. and J. V. Brackbill, BAAL: A Code for Calculating Three-Dimensional Fluid Flows at all Speeds with an Eulerian-Lagrangian Computing Mesh, Los Alamos Scientific Laboratory Report LA-6342 (1976).

27. Sani, R. L., P. M. Gresho and R. L. Lee, On The Spurious Pressure Generated By Certain GFEM Solutions Of The Incompressible Navier-Stokes Equations, Proc 3-rd Int. Conf. On Finite Elements Finite Elements In Flow Problems, Banff, Canada (1980).

28. Sani, R. L., P. M. Gresho, R. L. Lee and D. F. Griffiths, The Cause and Cure (?) Of The Spurious Pressures Generated By Certain FEM Solutions Of The Incompressible Navier-Stokes Equations, Part I, Int. J. Num. Methods In Fluids, 1, 17-43 (1981a).

29. Sani, R. L., P. M. Gresho, R. L. Lee, D. F. Griffiths and M. Engelman, The Cause and Cure (?) Of The Spurious Pressures Generated By Certain FEM Solutions Of The Incompressible Navier-Stokes Equations, Part II, Int. J. Num. Methods In Fluids, 1, 71-204 (1981b).

30. Sani, R. L., B. E. Eaton, P. M. Gresho, R. L. Lee and S. T. Chan, On The Solution Of The Time-Dependent Incompressible Navier-Stokes Equations Via A Penalty Galerkin Finite Element Method, Proc. Int. Conf. On Num. Meth. In Laminar and Turb. Flow, Venice, Italy (1981c).

31. Taylor, C. and P. Hood, A Numerical Solution Of The Navier-Stokes Equations Using Finite Element Technique, Computers and Fluids 1, 73-100 (1973).

32. Teman, R., Une Methode d'approximation de la Solution des Equations de Navier Stokes, Bull. Soc. Math., France, **96**, 115-152 (1968).

33. Teman, R., **Navier-Stokes Equations Theory and Numerical Analysis**, North Holland Publ. Co., Amsterdam (1977).

ınd Cure
ıs Of The
thods In

nan, The
tain FEM
I, Int. J.

'he Solu-
ıns Via A
Meth. In

es Equa-
, 73-100

tions de

ls, North